ORIGINAL ARTICLE

Self-tuning Control for Air Conditioning in a Room with Varying Temperature and Imperfectly Mixed Air

K. L. Ku[1] and T. S. Liu[1,*]

[1] *Department of Mechanical Engineering, National Chiao Tung University, Hsinchu 30010, Taiwan*

(**Received** 23 June 2015; **Accepted** 17 August 2015; **Published on line** 1 September 2016)

*Corresponding author: tsliu@mail.nctu.edu.tw

DOI: 10.5875/ausmt.v6i3.972

Abstract: This study aims to control indoor temperatures in an air-conditioned room to ensure the occupant's thermal comfort while minimizing energy consumption. In the literature, controlled simulations of air conditioning systems usually assume that the indoor air is perfectly mixed. This assumption provides little information on spatial temperature and air flow. By contrast, this study deals with imperfectly mixed air. A computational fluid dynamics method is used to model an air-conditioned room and links this model with controllers. A self-tuning controller can monitor plant changes based on recursive estimation and adjusts control parameters to meet desired performance. Therefore, this study develops self-tuning controllers to control room temperature. Disturbances of varying temperature are exerted to investigate control performance. This paper compares the performance of a self-tuning linear quadratic controller and a self-tuning proportional-integral-derivative (PID) controller. Simulation results show that both controllers track desired temperatures well. Compared with the self-tuning PID controller, the self-tuning linear quadratic controller yields less overshoot with a slower response. The proposed method in this study is validated by experimental results.

Keywords: imperfectly mixed air, room temperature control, self-tuning control

Introduction

Automatic control of air-conditioning systems can help improve thermal comfort and energy savings. The literature on controlled simulations assumes that indoor air is perfectly mixed [1, 2]. However, indoor air is in fact not perfectly mixed and rooms may feature significant temperature gradients. Computational fluid dynamic (CFD) models provide detailed information on a flow field. Therefore, the literature has focused on the development of CFD models [3] as the basis for designing air conditioner controllers [4]. CFD-based control simulations have the advantage of low costs in dealing with various conditions such as different climate conditions and different controllers.

A CFD method [5] is a numerical method used to solve fluid flow and heat transfer problems, whose fundamental equations are governed by Navier-Stokes equations. CFD can be used to describe the spatial-temporal distributions of temperature field, fluid velocity, pressure, and particle concentration. The distribution data are used to evaluate and optimize designs such as assessing thermal comfort under different operation conditions of air-conditioning systems [6]. Furthermore, visualization of data generated by a CFD method helps understand flow pattern and analyze fluid flow characteristics. In computer simulation, the coupling of a CFD model and a controller can validate control performance in simulated environments without restrictions of space and experimental devices.

To design model-based controllers, a mathematical description is required. There are two basic forms used: transfer functions and state-space equations. For control systems based on CFD numerical simulations, parameters and orders of transfer functions are commonly determined using mathematical identification techniques with certain criteria [4, 7] such as the coefficient of determination and Young identification criterion or using a data-based mechanistic method [8, 9]. State-space forms are established by discretizing energy equations based on finite volume schemes [10]. Since the state-

space model is a high-order model, the literature uses a proper orthogonal decomposition technique to obtain a reduced order thermal model in a room and this model is used to design controllers [10]. In addition, a velocity propagation method [11] has also been proposed to obtain thermal models for control design.

For control simulations in an air-conditioned room based on CFD modeling, most studies used a model predictive control [4, 8-10], genetic algorithm optimized neural proportional-integral-derivative (PID) control [11] or proportional-integral (PI) control [7]. Although self-tuning controllers can monitor plant changes through online system identification and control parameter tuning, few studies have investigated self-tuning controllers in an air-conditioned room established by CFD modeling. Moreover, model parameters in an air-conditioned room may change due to environmental variations or disturbances. Therefore, this study develops self-tuning controllers to control room temperature in an air-conditioned room in a way that integrates the controller into a CFD environment and evaluate temperature control performances under varying reference inputs and disturbances.

Integration of Indoor Thermal Model and Controllers

To integrate a controller and an indoor thermal model established by CFD, this study uses a CFD software, COMSOL, which is highly compatible with the control design software MATLAB/SIMULINK. SIMULINK can deal with partial differential equations based models through COMSOL [5]. Figure 1 depicts the proposed integrated framework. MATLAB is used to implement control algorithms and compute a control input which is imported to the CFD software and changes boundary conditions. CFD simulates heat transfer and flow dynamics according to physical equations, material properties, initial conditions, and boundary conditions.

K. L. Ku received his B.S. degree in Mechanical Engineering from National Central University in 2008. In the same year, he entered the Graduate School of National Chiao Tung University and studied in Mechanical Engineering Department. After he was in the first grade of master, he pursued his Ph.D. degree in National Chiao Tung University. His research interests include automatic control theory and control of air conditioning systems

T. S. Liu received his B.S. degree in 1979 from National Taiwan University, M.S. degree in 1982 from University of Iowa, and Ph.D. degree in 1986 from University of Iowa, all in mechanical engineering. Professor Liu has been teaching in National Chiao Tung University, Taiwan since 1987. His research interests include mechatronics and control.

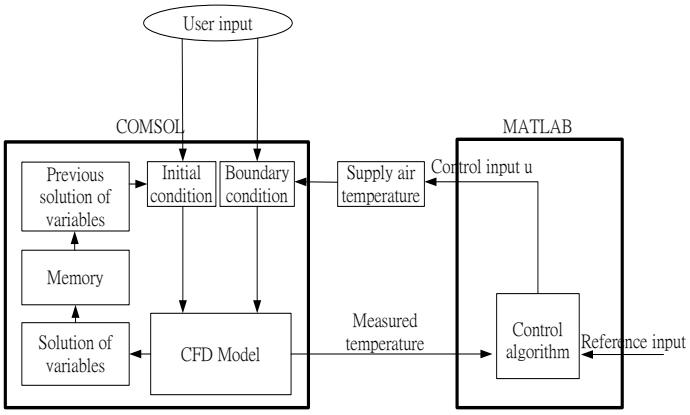

Figure 1. Integrated framework for designing controller with CFD modeling.

The temperature at a measurement point is fed back to a controller. A model geometry is built in CFD. At the beginning of the first time step, initial conditions and boundary conditions are defined by users. After the first time step, in each time step initial conditions are updated according to the previous solution stored in the memory of the CFD software and the boundary conditions are changed according to the control inputs.

In this study, digital self-tuning controllers are adopted in a CFD environment. The sampling period is prescribed as 10 s. The supply air temperature is treated as a control input and is applied at the inlet boundary.

Indoor Thermal Model

Navier-Stokes equations are used in this study to describe the temperature distribution in a room. Governing equations based on mass, momentum, and energy conservation are respectively are written as [12]

$$\frac{\partial \rho}{\partial t} + \nabla \cdot (\rho \vec{u}) = 0 \quad (1)$$

$$\rho \frac{\partial \vec{u}}{\partial t} + \rho(\vec{u} \cdot \nabla)\vec{u} = -\nabla\left[p + \mu\left(\nabla \vec{u} + (\nabla \vec{u})^T\right)\right] + \vec{F} \quad (2)$$

$$\rho c_p \frac{\partial T}{\partial t} + \rho c_p \vec{u} \cdot \nabla T = \nabla \cdot (k \nabla T) + Q \quad (3)$$

where ρ denotes the density, $\vec{u}$ the velocity vector, p the pressure, $\vec{F}$ the volume force; T the temperature, c_p the specific heat, k the heat conduction coefficient, and Q the heat source. The indoor air is assumed to be incompressible. Therefore, (1) can be rewritten as

$$\nabla \cdot \vec{u} = 0 \quad (4)$$

As depicted in Fig. 2, this study deals with a vertical plane in an air-conditioned room. The room is 5.80 m in width and 2.27 m in height. The measurement point in the

room is 0.7 m from the ground and 3.2 m from the left wall. An air conditioner is located 2.22 m from the ground on the left wall.

CFD simulations require the thermal and flow boundary conditions and initial conditions. As depicted in Fig. 2, the air inlet blows cool air from the air conditioner. The thermal and flow boundary conditions at the inlet are respectively defined as temperature and velocity. The inlet temperature or supply air temperature is treated as a control input in the control algorithm and is calculated by a controller. The inlet velocity is prescribed as 5.8 m/s and the angle of the velocity is 45° below the horizon. The position of return air in the air conditioner is prescribed as an air outlet. The thermal and flow boundary conditions at the outlet are defined as

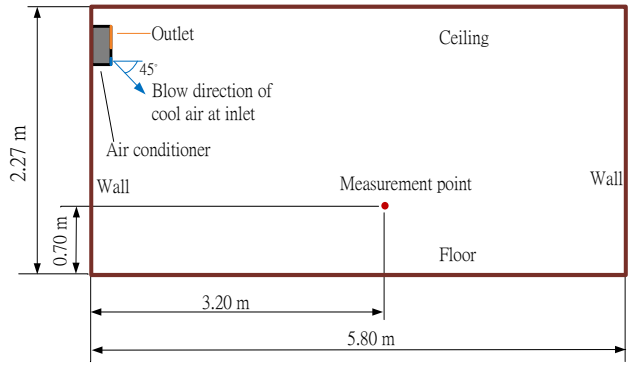

Figure 2. Dimension of an air-conditioned room.

Neumann conditions [5]. In Fig. 2, the thermal boundary conditions for the walls, ceiling, and floor are treated as temperature conditions. The temperature on both the ceiling and floor is prescribed as 30°C. Figure 3 shows the temperature variation of the walls. The flow boundary conditions on the walls, ceiling, and floor are treated as no-slip boundary conditions, where the velocity is prescribed as zero. The initial temperature and velocity of indoor air are respectively 30°C and 0 m/s. After defining the boundary conditions and initial conditions, the model is discretized by finite element mesh for subsequent computation.

To verify the simulation model, experiments are carried out and Figure 4 compares temperature variations at the measurement point in depicted Figure 2 between experimental data and simulation results. Both are found to be consistent. Temperature was measured using a Twintext TE-702D which provides a measurement range and accuracy are of -10.0 to 50.0 ℃ and ± 0.6 ℃, respectively.

Self-tuning Control

Self-tuning controllers provide adaptive control for plants whose parameters vary or are not completely known [13]. Such controllers combine online recursive system identification with a selected controller. A recursive least squares method is used to identify plant parameters which are then tuned based on the updated plant parameters and a control law. Figure 5 depicts the block diagram of a self-tuning controller.

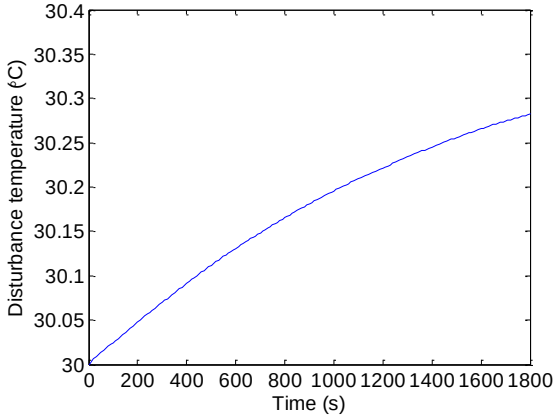

Figure 3. Temperature variation on the left and right walls due to environmental disturbances.

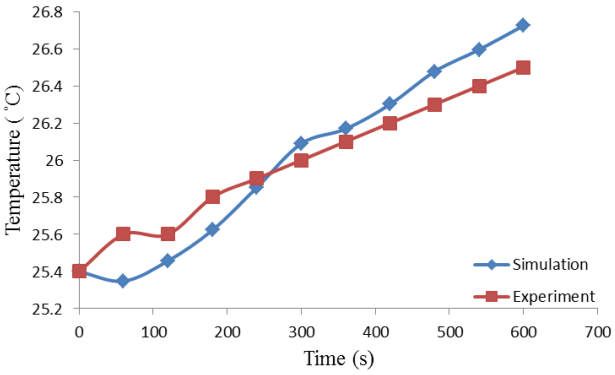

Figure 4. Comparison between experimental data and simulation results.

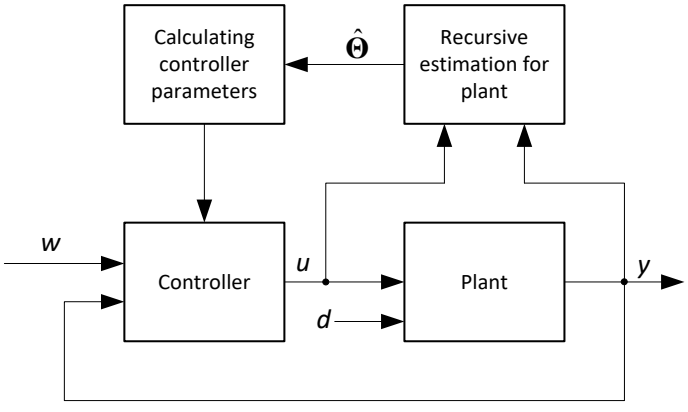

Figure 5. Block diagram of a self-tuning controller where *w* is a reference input, *u* is a control input, *y* is a plant output, *d* is a disturbance, and $\hat{\Theta}$ is an estimated model parameter.

To design a self-tuning controller, an autoregressive exogenous model (ARX) is expressed by

$$y(k) = \boldsymbol{\Theta}^T(k)\boldsymbol{\Phi}(k-1) + n(k) \quad (5)$$

where $y(k)$ is a plant output at the kth sample interval, $n(k)$ is a non-measurable random component, $\boldsymbol{\Theta}^T(k)$ is a parameter vector written as $\boldsymbol{\Theta}^T(k) = [a_1, a_2, .. a_{na}, b_1, b_2, ..., b_{nb}, d_1, d_2, ..., d_{nd}]$, and $\boldsymbol{\Phi}(k\text{-}1)$ is a regression vector written as $\boldsymbol{\Phi}^T(k\text{-}1)= [-y(k\text{-}1), -y(k\text{-}2), ..., -y(k\text{-}na), u(k\text{-}1), u(k\text{-}2), ...,u(k\text{-}nb)]$ where $u(k\text{-}1)$ is a control input at the $(k\text{-}1)$th sample interval.

Real plants usually differ from mathematical models used to describe them. In addition, model parameters are affected by the alteration of operating points and external disturbances. Thus, system identification is required. The commonly used method for parameter estimation is a recursive least square method. In recursive identification, new parameters are estimated using new measured data to update old estimated parameters. An exponential forgetting method [14] is presented, where the forgetting factor exponentially reduces the influence of old data on parameter estimation.

According to a recursive identification method [13, 15], the parameter vector is computed by

$$\hat{\boldsymbol{\Theta}}(k) = \hat{\boldsymbol{\Theta}}(k-1) + \frac{\mathbf{C}(k-1)\boldsymbol{\Phi}(k-1)}{1+\zeta(k-1)}\hat{e}(k) \quad (6)$$

where $\hat{e}(k) = y(k) - \hat{\boldsymbol{\Theta}}(k-1)\boldsymbol{\Phi}(k-1)$ is a prediction error, $\zeta(k-1) = \boldsymbol{\Phi}^T(k-1)\mathbf{C}(k-1)\boldsymbol{\Phi}(k-1)$ is an auxiliary scalar and $\mathbf{C}$ is a rectangular covariance matrix. If $\zeta(k-1) > 0$, then $\mathbf{C}(k)$ is computed by a recurrent algorithm

$$\mathbf{C}(k) = \mathbf{C}(k-1) - \frac{\mathbf{C}(k-1)\boldsymbol{\Phi}(k-1)\boldsymbol{\Phi}^T(k-1)\mathbf{C}(k-1)}{\varepsilon^{-1}(k\text{-}1) + \zeta(k-1)} \quad (7)$$

where

$$\varepsilon(k\text{-}1) = \phi(k) - \frac{1-\phi(k)}{\zeta(k-1)} \quad (8)$$

If $\zeta(k-1) = 0$, then $\mathbf{C}(k) = \mathbf{C}(k\text{-}1)$. A forgetting factor $\phi(k)$ is updated by the relation

$$\phi(k) = \left\{1 + (1+\rho)\left[\ln\left(1+\zeta(k-1)\right)\right] + \left[\frac{(\nu(k-1)+1)\eta(k-1)}{1+\zeta(k-1)+\eta(k-1)} - 1\right]\frac{\zeta(k-1)}{1+\zeta(k-1)}\right\}^{-1} \quad (9)$$

where ρ is a constant, $0 \le \rho \le 1$, $\eta(k) = \hat{e}^2(k) / \lambda(k)$, $\nu(k) = \phi(k)\left[\left(\nu(k-1)+1\right)\right]$, and

$$\lambda(k) = \phi(k)\left[\lambda(k-1) + \frac{\hat{e}^2(k-1)}{1+\zeta(k-1)}\right] \quad (10)$$

In this study, initial conditions for recursive identification are $\mathbf{C}(0)=10^3\mathbf{I}$, $\phi(0)=1$, $\lambda(0)=0.001$, $\nu(0)=10^{-6}$, and $\rho=0.99$. Assume that na and nb are 2 in the regression vector $\boldsymbol{\Phi}(k\text{-}1)$ in (5) and the order of the control plant is 2. Therefore, the transfer function of the plant can be written as

$$G(z^{-1}) = \frac{B(z^{-1})}{A(z^{-1})} = \frac{b_1 z^{-1} + b_2 z^{-2}}{1 + a_1 z^{-1} + a_2 z^{-2}} \quad (11)$$

where the parameters a_1, a_2, b_1 and b_2 are calculated by the recursive identification method.

The following subsections describe a PID controller and a linear quadratic controller. Both controllers are used in self-tuning controllers.

Self-tuning Proportional-integral-derivative Control

A PID controller [13] is the feedback control method extensively used in automatic control. The controller is composed of a proportion part, an integral part, and a derivative part and the controller output is the summation of the outputs of the three components.

This study adopts a PID controller [13] in the self-tuning PID controller and is written as

$$u(k) = K_p\left\{y(k-1) - y(k) + + \frac{T_s}{T_i}\left[w(k) - y(k)\right] + \frac{T_d}{T_s}\left[2y(k-1) - y(k) - y(k-2)\right]\right\} + u(k-1) \quad (12)$$

where $w(k)$ is a reference input, K_p is a proportion gain, T_i is an integral time constant, T_d is a derivative time constant, and T_s is a sampling period of 10 s. Three parameters of PID are determined by

$$K_p = 0.6K_{pu}\left(1 - \frac{T_s}{T_u}\right) \quad (13)$$

$$T_i = \frac{K_p T_u}{1.2K_{pu}} \quad (14)$$

$$T_d = \frac{3K_{pu}T_u}{40K_p} \quad (15)$$

where K_{pu} is an ultimate gain and T_u is an ultimate period. According to the relation of calculating the ultimate parameters for the second order model proposed by [13], if the condition

$$(1 - a_2 + a_1)^2 - 4 \le 0 \quad (16)$$

is satisfied, K_{pu} and T_u are determined by

$$K_{pu}=\frac{1-a_2}{b_2}, \mathrm{T}_u=\frac{2\pi T_s}{\cos^{-1}((a_2-1-a_1)/2)} \tag{17}$$

If the condition (16) is not satisfied, K_{pu} and T_u are determined by

$$K_{pu}=\frac{a_1-a_2-1}{b_2-b_1}, \mathrm{T}_u=2T_s \tag{18}$$

K_{pu} and T_u are computed in every sampling period according to updating identified parameters.

Self-tuning Linear Quadratic Control

A linear quadratic controller [15] attempts to find the control action such that a quadratic performance criterion J is minimized:

$$J=\sum_{k=0}^{\infty}\left\{ \left[w(k)-y(k)\right]^2+q_u\left[u(k)\right]^2\right\} \tag{19}$$

where $q_u \geqq 0$ is a penalization constant, which penalizes the control input so as to reduce energy consumption inside an air-conditioned room. In this study, q_u is prescribed as 0.01. If the model is designed based on a polynomial input-output model, the block diagram is depicted in Fig. 6, where $P(z^{-1})$, $Q(z^{-1})$, and $R(z^{-1})$ denote polynomials for the controller that contains a feedback part and a feedforward part.

Based on the minimum criterion (19), the control parameters $P(z^{-1})$, $Q(z^{-1})$, and $R(z^{-1})$ are obtained by performing the spectral factorization and solving two polynomial equations [16]. The spectral factorization $D(z^{-1})$ is a polynomial and satisfies [15]

$$A(z^{-1})q_uA(z)+B(z^{-1})B(z)=D(z^{-1})\cdot\delta\cdot D(z) \tag{20}$$

where $A(z^{-1})=1+a_1z^{-1}+a_2z^{-2}$ and $B(z^{-1})=b_1z^{-1}+b_2z^{-2}$ are polynomials of the control plant, $D(z^{-1})=d_0+d_1z^{-1}+d_2z^{-2}$ is the spectral factorization, and δ is a constant so that $d_0=1$ in this study. In addition, conditions based on the Routh stability criterion

$$1-d_2^2>0 \tag{21}$$
$$(1+d_2)^2-d_1^2>0 \tag{22}$$

have to be satisfied for the stability of the polynomial $D(z^{-1})$. By solving (20), (21), and (22), constants of d_1 and d_2 in $D(z^{-1})$ are computed by

$$d_1=\frac{m_1}{\delta+m_2} \tag{23}$$
$$d_2=\frac{m_2}{\delta} \tag{24}$$

where

$$\delta=\frac{\lambda+\sqrt{\lambda^2-4m_2^2}}{2} \tag{25}$$
$$\lambda=\frac{m_0}{2}-m_2+\sqrt{\left(\frac{m_0}{2}+m_2\right)^2-m_1^2} \tag{26}$$
$$m_0=q_u(1+a_1^2+a_2^2)+b_1^2+b_2^2 \tag{27}$$
$$m_1=q_u(a_1+a_1a_2)+b_1b_2 \tag{28}$$
$$m_2=q_ua_2 \tag{29}$$

Polynomials $P(z^{-1})$ and $Q(z^{-1})$ in Fig. 6 are the solution of the equation [15]:

$$A(z^{-1})P(z^{-1})+B(z^{-1})Q(z^{-1})=D(z^{-1}) \tag{30}$$

where $P(z^{-1})=p_0+p_1z^{-1}$ and $Q(z^{-1})=q_0+q_1z^{-1}$ in this study. Constants p_0, p_1, q_0, and q_1 are determined by solving (30). Moreover, polynomial $R(z^{-1})$ is determined by solving

$$D_w(z^{-1})S(z^{-1})+B(z^{-1})R(z^{-1})=D(z^{-1}) \tag{31}$$

where $D_w(z^{-1})$ denotes a polynomial denominator of a reference input $w(z^{-1})$ and $S(z^{-1})$ is a by-product, which doesn't need to be calculated in the tuning process. Since the reference input is a step input in this study, $D_w(z^{-1})=1-z^{-1}$. After $P(z^{-1})$, $Q(z^{-1})$, and $R(z^{-1})$ are determined by using (30) and (31), based on Fig. 6, the control input $u(k)$ is formulated as

$$u(k)=\frac{R(z^{-1})}{P(z^{-1})}w(k)-\frac{Q(z^{-1})}{P(z^{-1})}y(k) \tag{32}$$

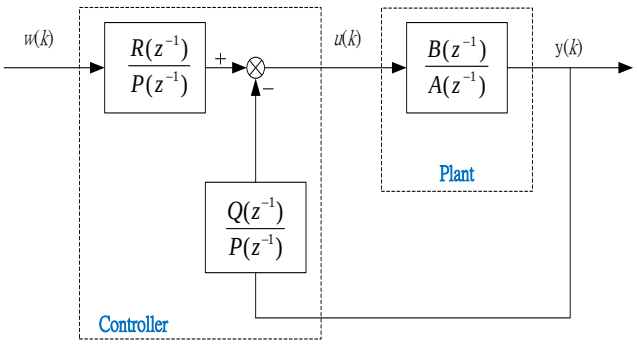

Figure 6. Block diagram of a linear quadratic controller with a plant.

Simulation Results of Self-tuning Controllers

Control simulations were conducted to evaluate the performance of the self-tuning controllers. The lower bound of the control input is prescribed as 18°C. The desired reference temperature trajectory is initially defined as 26°C with step changes to 27°C at 10 min and 25°C at 20 min. Two disturbances are exerted to evaluate controller effectiveness. One disturbance represents an estimated temperature variation near two walls due to heat transfer through the walls from outside. Figure 3 depicts the temperature variation due to the disturbance. The other disturbance is exerted to account for unsteady operating conditions of the air conditioner and is prescribed as +1°C of the supply air temperature from 830 s to 1030 s. Figure 7 compares temperature responses of self-tuning controllers in the room subjected to disturbances.

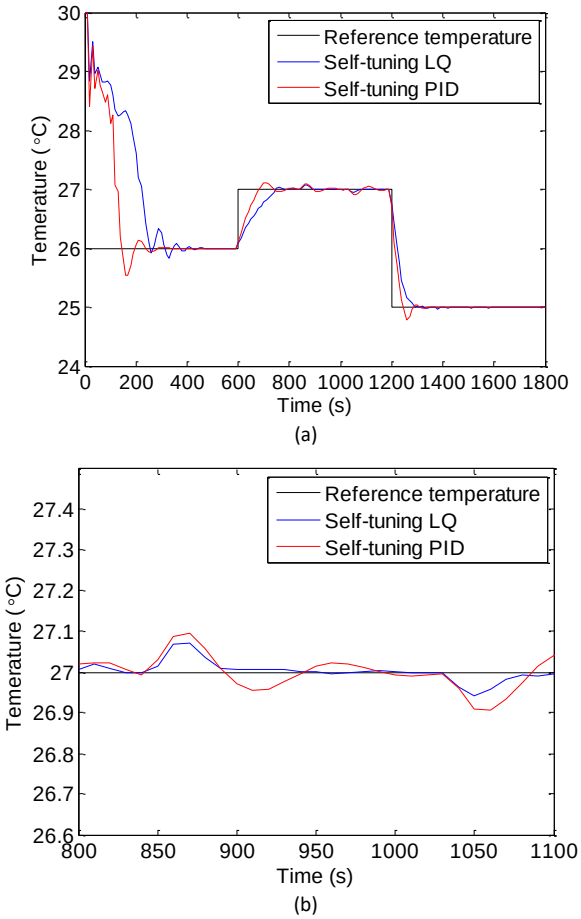

Figure 7. (a) Overall temperature responses and (b) partial enlargement responses by using self-tuning LQ and self-tuning PID controllers at the measurement point in a room subjected to disturbances.

In Fig. 7(a), there is a little overshoot following the first reference temperature of 26°C. However, the self-tuning PID controller yields less overshoot in the later step up and step down of the reference temperature. The self-tuning LQ control almost has no overshoot in the later step up and step down of the reference temperature. The overshoots of both self-tuning controllers during the period of the first reference temperature of 26°C are larger than that of the later reference temperatures because the self-tuning controllers need more time steps to approach plant parameters. In Fig. 7(b), although the supply air temperature is subject to disturbances, the self-tuning controllers keep the temperature close to the reference temperature and just have a little oscillation since the controllers can quickly compensate the effect of disturbances. The overall system responses demonstrate that the self-tuning controller can follow the reference temperature even if the thermal model is nonlinear and disturbances exist. A comparison of results shows that the self-tuning PID controller responds faster than the self-tuning LQ controller. However, both settling times are close except during the period of the first reference temperature of 26°C. Furthermore, the LQ controller yields less overshoot in transient response and less oscillation under the influence of the disturbances.

Variations of the supply air temperature shown in Fig. 8 influence the pattern of the temperature distributions at 1800 s depicted in Fig. 9, because the variations of the supply air temperature influence air thermal convection, which in turn affects air flow and thus the pattern of temperature distribution. If the supply air temperature is lower, a temperature difference between the supply air temperature and wall temperature will increase and air convection will become stronger. In Fig. 8, at 1800 s the supply air temperature of the self-tuning PID controller is lower than the self-tuning LQ controller. As a result, Fig. 9 shows that the LQ controller and PID controller yield opposite temperature distributions, where the PID controller results in a lower supply air temperature and hence a cooler zone far from the air conditioner, while the LQ controller results in a higher supply air temperature and hence a cooler zone near the air conditioner.

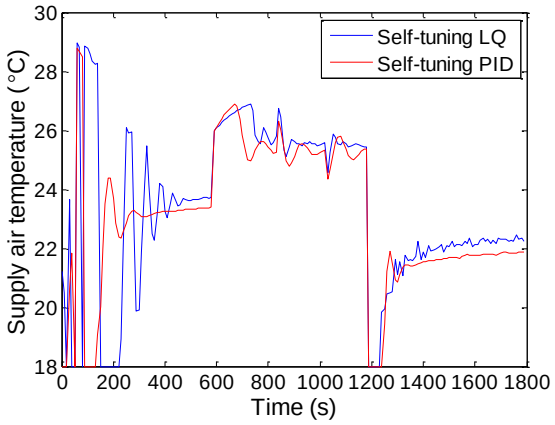

Figure 8. Comparison of supply air temperatures treated as control input using between self-tuning LQ and self-tuning PID controllers.

Although this study is focused on a small room, the proposed method can also be extended to deal with large rooms such as auditoriums by first modifying the model geometry and increasing the number of finite elements. Although the temperature distribution may differ with room size and geometry and it may take longer time to reach steady state temperature for large rooms, the temperature can be kept around the reference temperature by means of adapting the self–tuning controllers.

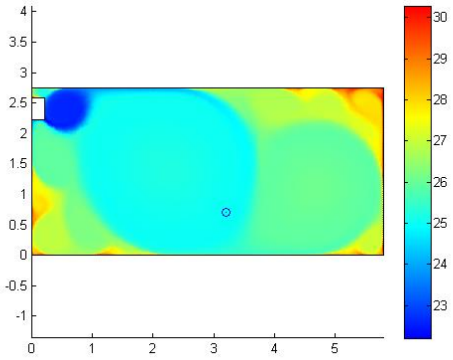

(a)

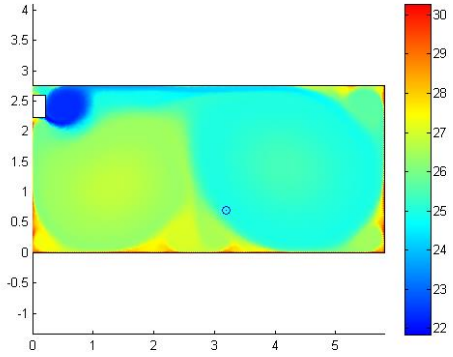

(b)

Figure 9. Temperature distributions at 1800 s in a room resulting from (a) self-tuning LQ controller and (b) self-tuning PID controller in Figure

To investigate effects of different outlet positions, the outlet position was moved to a lower right corner in Fig. 10(a), and Fig. 11(a) shows that the temperature oscillations and overshoots of both controllers are larger than those depicted in Fig. 7(a) resulting from the original outlet position. However, the temperature responses can still be regulated around the reference temperature. Moreover, if the outlet position is located at a lower left corner as in Fig. 10(b), Fig. 11(b) shows that the LQ controller also yields good control performance. The response of the LQ controller is smooth and has less oscillation. And the LQ controller yields no overshoot except during the period of the first reference temperature of 26°C. Compared with Fig. 7(a) with the original outlet position, when the outlet position is changed to the lower left corner, the PID controller yields larger oscillation and overshoot during the period of the first reference temperature of 26°C. However, the overshoot and oscillation are reduced during the period of later reference temperatures. In addition, the temperature response using the PID controller can be kept around the reference temperature.

(a)

(b)

Figure 10. The same room as Figure 2 but the outlet position is moved to (a) the lower right corner and (b) the lower left corner.

Conclusion

To achieve thermal comfort, this study coupled self-tuning PID and LQ controllers with CFD modeling. Simulation results show that both self-tuning controllers perform well in the inherent nonlinear model with disturbances exerted on the boundary and a varying reference input. This results from the adaptability of self-tuning controllers. The controllers can adequately monitor parameter changes and adjust control parameters. Concerning transient behavior, the self-tuning LQ controller yields less overshoot and slower response than the self-tuning PID controller. This is attributed to the penalization factor, as depicted in (19), in the LQ controller. Experimental results shown in Fig. 4 validate the present model. If the outlet position is moved to the lower right or the lower left corner, the self-tuning controllers yield larger oscillation and overshoot than those resulting from the original outlet position. However, responses of self-tuning LQ controller with the outlet at the lower left corner are as good as those from the original outlet position. In addition, the temperature responses can still be regulated around the reference temperature by the self-tuning controllers when the outlet position is changed.

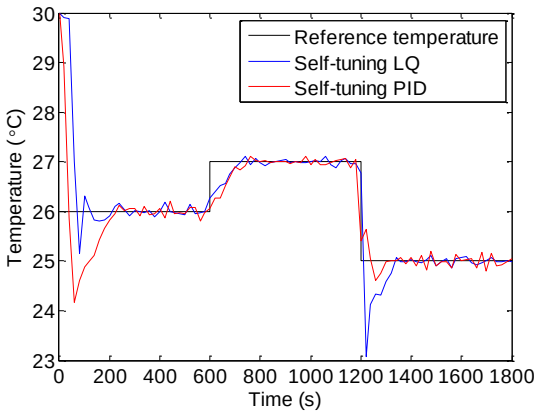

Figure 11. Temperature responses by using the self-tuning LQ and PID controllers when the outlet position is located at (a) the lower right corner and (b) the lower left corner.

References

[1] B. Tashtoush, M. Molhim, and M. Al-Rousan, "Dynamic model of an HVAC system for control analysis," *Energy*, vol. 30, no. 10, pp. 1729-1745, 2005. doi: 10.1016/j.energy.2004.10.004

[2] A. S. Kalagasidis, P. Weitzmann, T. R. Nielsen, R. Peuhkuri, C.-E. Hagentoft, and C. Rode, "The international building physics toolbox in Simulink," *Energy and Buildings*, vol. 39, no. 6, pp. 665-674, 2007. doi: 10.1016/j.enbuild.2006.10.007

[3] Y.-B. Li, G.-X. Sun, and X.-C. Wang, "Temperature field-wind velocity field optimum control of greenhouse environment based on CFD model," *Mathematical Problems in Engineering*, vol. 2014, no. 2014, Article ID 949128, 2014. doi: 10.1155/2014/949128

[4] T. Z. Desta, K. Janssens, A. Van Brecht, J. Meyers, M. Baelmans, and D. Berckmans, "CFD for model-based controller development," *Building and Environment*, vol. 39, no. 6 , pp. 621-633, 2004. doi: 10.1016/j.buildenv.2004.01.001

[5] A. W. M. van Schijndel, "Integrated modeling of dynamic heat, air and moisture processes in buildings and systems using Simulink and COMSOL," *Building Simulation*, vol. 2, no. 2, pp. 143–155, 2009. doi: 10.1007/s12273-009-9411-x

[6] Y.-T. Chou, S.-Y. Hsia, and B.-W. Lee, "Efficiency enhancement on thermal comfort assessment of indoor space with air-conditioner using computational analysis," *Mathematical Problems in Engineering*, vol. 2014, Article ID 739619, 2014. doi: 10.1155/2014/739619

[7] Q.-L. Meng, Y. Wang, X.-Y. Yan, and Z.-Q. Li, "CFD assisted modeling for control system design: A case study," *Simulation Modelling Practice and Theory*, vol. 17, no. 4, pp. 730-742, 2009. doi: 10.1016/j.simpat.2009.01.003

[8] A. Van Brecht, S. Quanten, T. Zerihundesta, S. Van Buggenhout, and D. Berckmans, "Control of the 3-D spatio-temporal distribution of air temperature," *International Journal of Control*, vol. 78, no. 2, pp. 88-99, 2005. doi: 10.1080/00207170500036118

[9] T. Z. Desta, A. Van Brecht, J. Meyers, M. Baelmans, and D. Berckmans, "Numerical simulation and controller development for energy transfer in imperfectly mixed fluids," *Indoor and Built Environment*, vol. 14, no. 5, pp. 371-380, 2005. doi: 10.1177/1420326X05057467

[10] K.-J. Li, H.-Y. Su, J. Chu, and C. Xu, "A fast-POD model for simulation and control of indoor thermal environment of buildings," *Building and Environment*, vol. 60, pp. 150-157, 2013. doi: 10.1016/j.buildenv.2012.11.020

[11] Z.-H. Song, B. T. Murray, and B. Sammakia, "A dynamic compact thermal model for data center analysis and control using the zonal method and artificial neural networks," *Applied Thermal Engineering*, vol. 62, no. 1, pp. 48-57, 2014. doi: 10.1016/j.applthermaleng.2013.09.006

[12] Comsol Multiphysics, Comsol Multiphysics–CFD Module Users' Manuals, pp. 112-194, 2013.

[13] V. Bobal, J. Bohm, and R. Prokop, "Practical aspects of self-tuning controllers," *International Journal of Adaptive Control and Signal Processing*, vol. 13, no. 8, pp. 671-690, 1999.

[14] R. Kulhavy, "Restricted exponential forgetting in real-time identification," *Automatica*, vol. 23, no. 5, pp. 589-600, 1987. doi: 10.1016/0005-1098(87)90054-9

[15] V. Bobál, J. Böhm, J. Fessl, and J. Macháček, *Practical aspects of self-tuning controllers: Algorithms, implementation and applications.* Springer-Verlag, London, pp. 32-159, 2005.

[16] M. Sebek and V. Kucera, "Polynomial approach to

quadratic tracking in discrete linear systems," *IEE Transactions on Automatic Control*, vol. 27, no. 6, pp. 1248-1250, 1982.
doi: 10.1109/TAC.1982.1103089